Physica A 392 (2013) 1694–1701

Contents lists available at SciVerse ScienceDirect

Physica A

journal homepage: www.elsevier.com/locate/physa

Characterization of nanostructured material images using fractal descriptors

João B. Florindo [a], Mariana S. Sikora [b], Ernesto C. Pereira [b], Odemir M. Bruno [a,*]

[a] Physics Institute of São Carlos, University of São Paulo, São Carlos, Brazil

[b] Interdisciplinary Electrochemistry and Ceramics Laboratory, Federal University of São Carlos, São Carlos, Brazil

ARTICLE INFO

Article history:
Received 30 June 2012
Received in revised form 9 October 2012
Available online 20 December 2012

Keywords:
FEG images
Nanoscale materials
Pattern recognition
Fractal dimension
Fractal descriptors
Image analysis

ABSTRACT

This work presents a methodology to the morphology analysis and characterization of nanostructured material images acquired from FEG-SEM (Field Emission Gun-Scanning Electron Microscopy) technique. The metrics were extracted from the image texture (mathematical surface) by the volumetric fractal descriptors, a methodology based on the Bouligand–Minkowski fractal dimension, which considers the properties of the Minkowski dilation of the surface points. An experiment with galvanostatic anodic titanium oxide samples prepared in oxalyc acid solution using different conditions of applied current, oxalyc acid concentration and solution temperature was performed. The results demonstrate that the approach is capable of characterizing complex morphology characteristics such as those present in the anodic titanium oxide.

1. Introduction

The morphology analysis of solid samples is an important research area in Materials Science to characterize some of their properties [1–4]. Generally, the technique employed in this kind of application consists in the quantitative analysis of the micrographs obtained using one (or more) of the following techniques, such as FEG-SEM (Field Emission Gun-Scanning Electron Microscopy), AFM (Atomic Force Microscopy), STM (Scanning Tunneling Microscopy) or TEM (Transmission Electron Microscopy). In any case, the results are a matrix of values which expresses the topography of the measured sample.

When the morphology of the material is investigated, we observe that each image presents a specific distribution pattern. This distribution is quite similar to that found in textures classically studied with image analysis tools, e.g., the so-called texture analysis methods [5]. Of course, the quantitative analysis of nanostructured materials is easy to perform for well behaved samples which have been described using simple functions of existing software packages. One example is the automatic counting of pores in self-organized anodic porous alumina [1] using ImageJ [6] and Gwyddion [7]. The problem is different when studying complex morphology characteristics of the samples as those ones where the distinction among the patterns is not obvious. In this case, a more sophisticated analysis must be used and these are generally are not included in those software packages described above.

Among the methods described in the literature, those ones based on fractal analysis have presented excellent performance in the investigation of complex textures, mainly on those synthesized and natural samples [8–11]. Actually, nature is rich in self-similar patterns, that is, structures which repeat themselves under different scales. From a mathematical point of view, this is also an intrinsic property of fractal objects. Therefore, fractal geometry is appropriate to measure such kind of structures and, as consequence, self-similarity also measures complexity (meaning the level of details along scales) which is directly related to spatial occupation in the structure.

* Corresponding author.
E-mail address: bruno@ifsc.usp.br (O.M. Bruno).

0378-4371/$ – see front matter © 2012 Elsevier B.V. All rights reserved.
doi:10.1016/j.physa.2012.11.020

Table 1
Experimental matrix for the anodic titanium oxide samples preparation using a factorial design procedure.

Experiments	Current density/mA cm^{-2}	Temperature/°C	Concentration/mol L^{-1}
1	10	10	0.05
2	20	10	0.05
3	10	30	0.05
4	20	30	0.05
5	10	10	0.5
6	20	10	0.5
7	10	30	0.5
8	20	30	0.5

Not withstanding that fractal dimension provides a good solution in many object identification problems, it is limited in the representation of some classes of objects [12] due to two main aspects: (i) fractal dimension is a real number which is insufficient to characterize such objects. (ii) there are samples that have different patterns but present the same fractal dimension. In fact, these objects can have a more or less self-similar aspect depending on the scale observed [13]. In the literature, different propositions have been presented to solve the above drawbacks. The main ones are multifractal [14], multiscale fractal dimension [15] and fractal descriptors [9]. Considering that several papers have demonstrated the superior performance of fractal descriptors dealing with texture images over the other ones, we are focused here on such an approach as a tool for texture discrimination [9,10,5,11].

We apply Volumetric Minkowski descriptors methodology, which was initially developed in Ref. [8]. It is derived from the Bouligand–Minkowski fractal dimension. The descriptors are obtained by mapping the original gray level image (of FEG-SEM data, in this case) onto a three-dimensional mathematical surface. Thus, such a surface is dilated by the Bouligand–Minkowski method using spheres with predefined radii. The fractal descriptors are then estimated from the volume of dilation for each sphere radius. With the growing of the dilation radius, the spheres start to interfere among themselves, forming a wavefront which is tightly related to the structure of the material. It is important to stress that the dilation process captures the arrangement of the topography [8]. Thus, these descriptors are capable of providing very rich information about the morphology of the material and, consequently, are a strong method for a nanostructured material characterization task. The use of the Volumetric Fractal Descriptors applied to nanostructured surfaces was initially proposed in Ref. [16]. In that seminal project, it was suggested that Fractal Volumetric Descriptors could be used to characterize and analyze such nanostructures, showing the discrimination power on two distinct conditions. In the present work, an experiment with galvanostatic anodic titanium oxide samples prepared in oxalyc acid solution using eight different conditions of applied current, oxalyc acid concentration and solution temperature was performed, and demonstrates that the proposed technique is capable of identifying the nanosurfaces. The nature of the material's surfaces and its images are a difficult problem in image analysis, and the proposed technique demonstrates itself to be suitable to characterize and to identify nanostructured surfaces.

2. Materials and methods

2.1. Materials

The samples used in this work were galvanostatic anodic titanium oxide ones prepared in oxalyc acid solution. In this electrochemical preparation method, a titanium plate is the anode in a two electrode electrochemical cell. A platinum plate was used as a cathode. Then, the anode is polarized under constant current condition and an oxide film starts to form over the anode following the equation: $Ti + 2H_2O \rightarrow TiO_2 + 4H^+ + 4e^-$. It is important to stress that TiO_2 is formed by the direct reaction between the metal and water over the metal. The surface morphology of the oxide is sensible to the experimental conditions used. In the present case, different values of applied current, oxalyc acid concentration and solution temperature were used as described in Table 1. Using a 2^3 factorial design [17], 8 titanium oxide anodizations were performed, generating, therefore, 8 classes of samples. From each class, 8 images from different regions on their surface were acquired. Therefore, we have a total of 64 samples to be used in the model building. Each sample is a rectangular piece of the plate, which is measured through SEM-FEG technique generating a matrix (image) with a resolution of 3072 $\times$ 2060 pixels. Fig. 1 shows one image per class, illustrating the general aspect of the dataset.

3. Results

3.1. Fractal theory

Fractals are objects formally defined as a set of points whose Hausdorff–Besicovitch dimension (see the concept below) exceeds strictly the Euclidean dimension. In practice, it is an object generated through a dynamic system that presents infinite complexity and self-similarity [13]. Here, complexity states for the level of details under different scales.

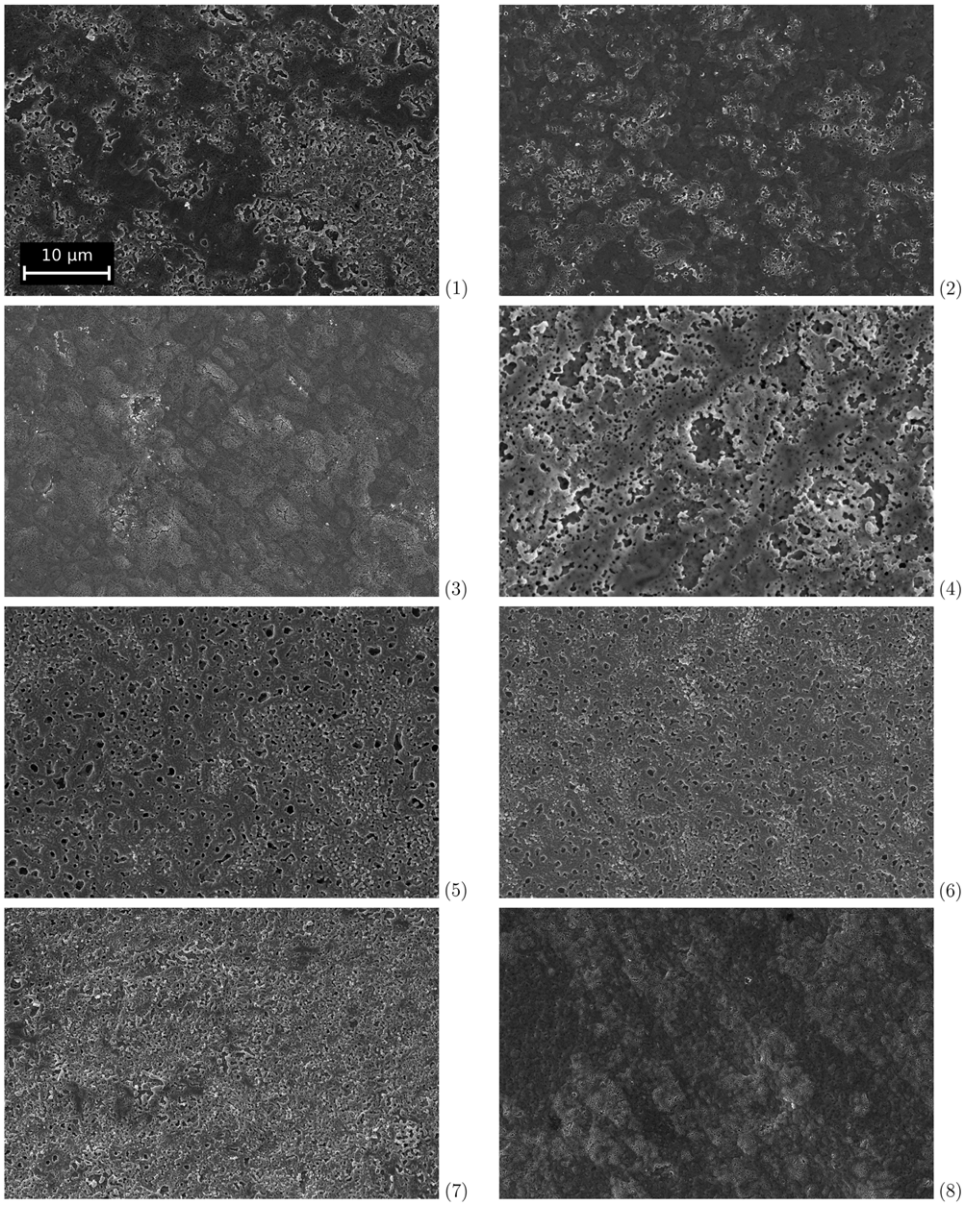

Fig. 1. Titanium oxide dataset. Each image number corresponds to the same number of the experiments column presented in Table 1.

Self-similarity expresses the fact that if one takes the fractal under different observation scales, he will observe the repetition of patterns only changed by simple geometrical transforms (affine transforms). It is important to stress that these properties are observed at infinite scale. In nature, we can find a lot of objects which present self-similarity and complexity at certain levels. Then, this is a strong motivation to approximate these structures through fractal metric. The most frequently used of such fractal metrics is the one called fractal dimension.

3.1.1. Fractal dimension

The first concept presented in the literature of fractal dimension [13] is the same one as Hausdorff dimension, which is based on the Hausdorff measure $\mathfrak{H}_\delta^s$ concept. Let A be a subset of $\Re^n$ and s and δ non-negative real values. Then:

$$\mathfrak{H}_\delta^s(A) = \inf\left\{\sum \|U_i\|^s \text{ such that } \{U_i\} \text{ is a } \delta\text{-cover of } A\right\}, \tag{1}$$

where $\{U_i\}$ is a δ-cover of A if $A \subset \bigcup_{i=1}^{\infty} U_i$, being $0 < \|U_i\| \leq \delta$.

The Hausdorff s-measure $\mathfrak{H}^s$ is given by:

$$\mathfrak{H}^s(A) = \lim_{\delta \to 0} \mathfrak{H}_\delta^s(A). \tag{2}$$

An interesting and important characteristic of this measure is that $\mathfrak{H}^s(A)$ is always 0 for any $s < d_H$ and ∞ for any $s > d_H$. The real value d_H is the so-called Hausdorff dimension of A, that is:

$$d_H(X) = \inf\left\{s|H^s(X) = 0\right\} = \sup\left\{s|H^s(X) = \infty\right\}. \tag{3}$$

A special case of fractal dimension definition is the Bouligand–Minkowski (BM) dimension, described in the following section.

3.1.2. Bouligand–Minkowski

As well as in the Hausdorff dimension, BM also has an associated measure, which is, in this case, an upper measure $\overline{q_\tau}$ and a lower one $\underline{q_\tau}$ defined through:

$$\overline{q_\tau}(X, R) = \liminf_{r\to 0} q_\tau(X, R, r), \tag{4}$$

$$\underline{q_\tau}(X, R) = \limsup_{r\to 0} q_\tau(X, R, r), \tag{5}$$

where

$$q_\tau(X, R, r) = \frac{V(\partial X \oplus rR)}{r^{n-\tau}}, \tag{6}$$

with $-\infty < \tau < \infty$, $r > 0$, ∂X is the boundary of X and $\oplus$ denotes the morphological dilation by an element R with radius r.

The upper and lower dimension, $\overline{D_B}$ and $\underline{D_B}$ respectively, are defined by:

$$\overline{D_B}(X, R) = \inf\{\tau|\overline{q_\tau}(X, R) = 0\}, \tag{7}$$

$$\underline{D_B}(X, R) = \inf\{\tau|\underline{q_\tau}(X, R) = 0\}. \tag{8}$$

In a discrete space, like that of digital images here analyzed, the direct application of the above equations is not viable. In such situations, a common practice is to employ neighborhood techniques. Particularly, here, we are interested in the estimation of dimension in $\Re^3$. In this space, the BM dimension may be presented through:

$$D_B(X) = \lim_{r\to 0}\left(3 - \frac{\log(V(\partial X \oplus Y_r))}{\log r}\right), \tag{9}$$

where V is the volume of the dilated structure and Y_r is an Euclidean sphere with radius r.

3.1.3. Fractal descriptors

As described in the Introduction, the fractal dimension is a scalar value and it is not enough to characterize such complex structures as those presented in Fig. 1. Therefore, we have developed an improved concept related to fractal dimension which is not a real number but a vector [12]. This mathematical object was called a fractal descriptor and its fundamental aspects are described in the following paragraphs [9,10,5,11].

We propose to extract the morphological properties from the samples through an analysis based on fractal geometry of the FEG images. In this way, an initial procedure is to estimate the fractal dimension of the data represented in FEG samples using the above Bouligand–Minkowski method due to its precision [18,11,8]. We applied a neighborhood approach once the FEG image is described in a discrete space.

The most intuitive way of calculating fractal dimension of a FEG image is to map the data onto a 3D gray intensity surface. The Fig. 2 shows an example of the image presented as a 3D gray surface. This is performed in a simple manner by representing the image $I \in [1 : M] \times [1 : N] \to \Re$ in the surface S

$$S = \{i, j, f(i, j)|(i, j) \in [1 : M] \times [1 : N]\}, \tag{10}$$

and

$$f(i, j) = \{1, 2, \ldots, \text{max\_value}|f = I(i, j)\}, \tag{11}$$

being max_value the maximum value in the FEG data.

A classical way of calculating the BM dimension of a surface in discrete space is dilating it with spheres varying the radius r, which is presented in Fig. 3. This figure illustrates the dilation process for two different values of r. Using this approach, we compute the dilation volume $V(r)$ (number of points inside the dilated surface) for each value of r. The dimension is given through:

$$D_B = 3 - \lim_{r\to 0}\frac{\log(V(r))}{\log(r)}. \tag{12}$$

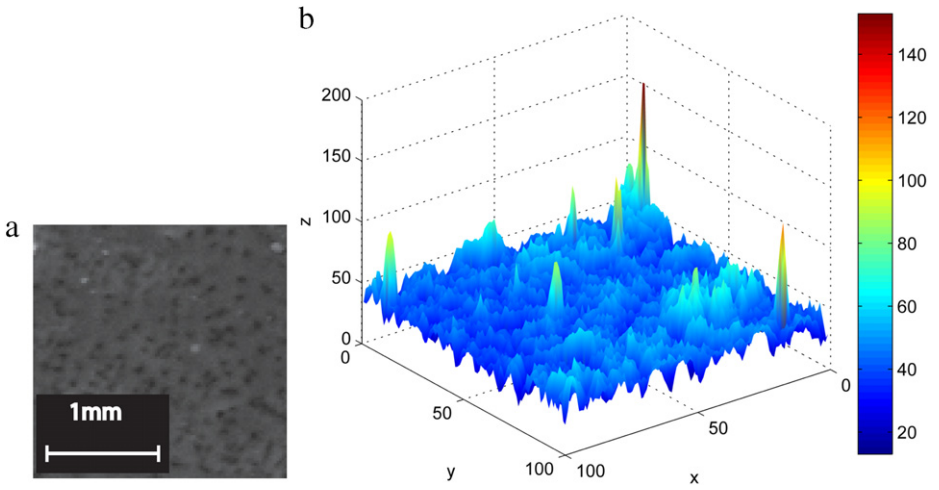

Fig. 2. Texture image mapped onto a 3D surface. (a) Plain image. (b) Surface, obtained considering the gray levels as z axis.

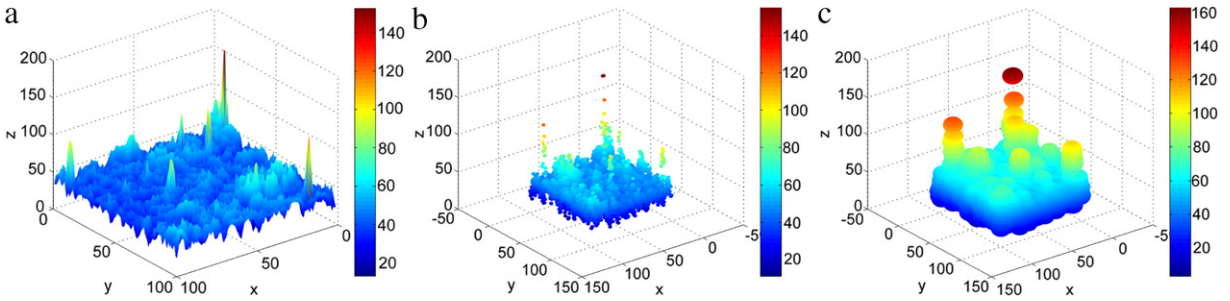

Fig. 3. Dilated surfaces with different radii. (a) Original surface. (b) Radius 2. (c) Radius 10.

For computational efficiency, a usual solution to calculate $V(r)$ is to employ the exact Euclidean Distance Transform (EDT) [19], which is for a surface S in three dimensions given by:

$$\mathrm{EDT}(p) = \min\{d(p, q) | q \in U \setminus S\}, \tag{13}$$

where d is the Euclidean distance and $U \setminus S$ corresponds to the complement of S taken over a cube U (universal set) which contains S. When we are dealing with exact EDT, the distance has predefined values:

$$E = 0, 1, \sqrt{2}, \ldots, l, \ldots, \tag{14}$$

where

$$l \in D = \{d | d = (i^2 + j^2)^{1/2}; i, j \in \mathbb{N}\}. \tag{15}$$

Initially, we define the set $g_r(S)$ of points at a distance r from S:

$$g_r(S) = \left\{(x, y, z) | [(x - S_x)^2 + (y - S_y)^2 + (z - S_z)^2]^{1/2} = E(r)\right\}, \tag{16}$$

where S_x, S_y, S_z are the coordinates of points in S.

The dilation volume $V(r)$ is given by:

$$V(r) = \sum_{i=1}^{r} Q(i), \tag{17}$$

where $Q(i)$ is provided through the following expression:

$$Q(i) = \sum_{(x,y,z) \in U} \chi_{g_r}(x, y, z), \tag{18}$$

where χ states for the indicator function.

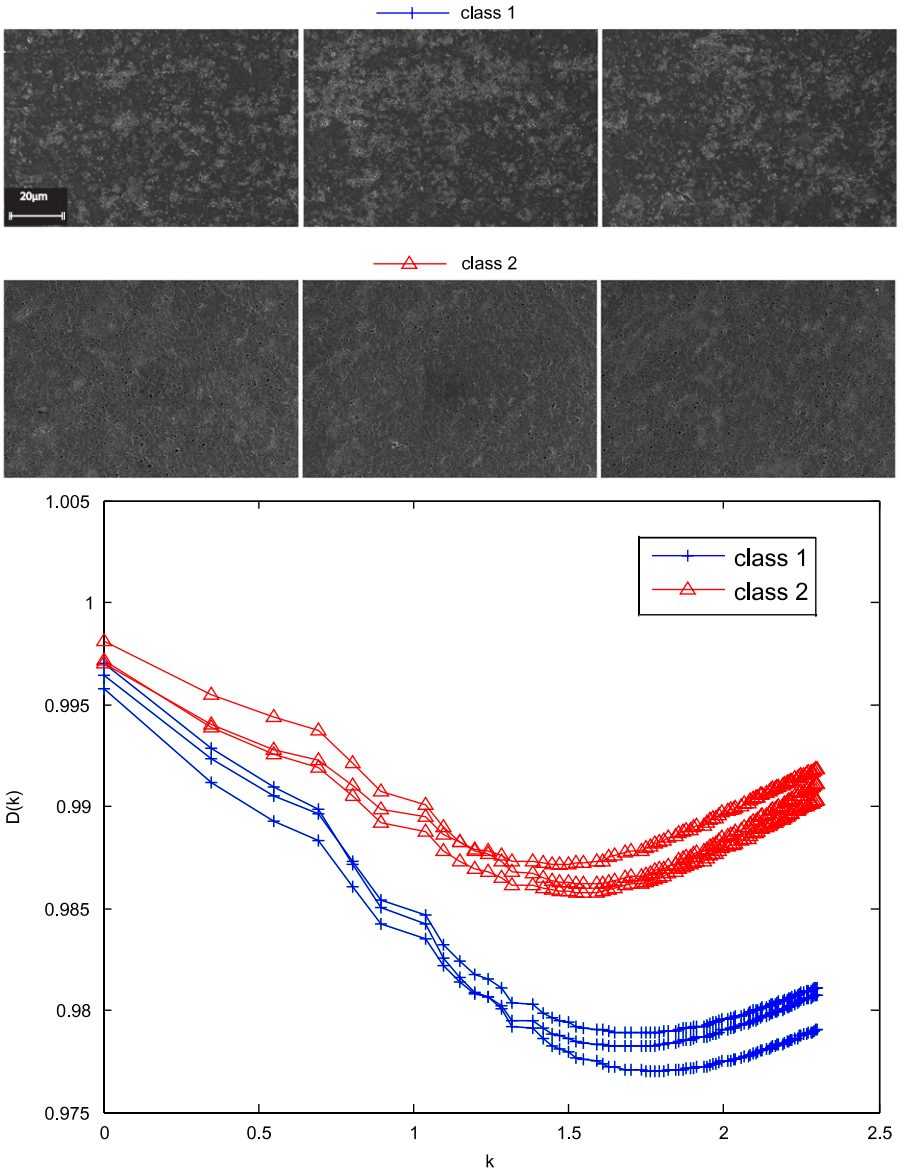

Fig. 4. Discrimination performance of proposed descriptors.

Therefore, $V(r)$ and r present a power law relation. The descriptors themselves are obtained using the following relation u:

$$u : \log(r) \rightarrow \log(V(r)), \tag{19}$$

where V acts as a fractality measure and r is the scale parameter.

4. Discussion

Several times, to extract the information from function u, a mathematical space transformation is necessary, such as Fourier or Principal Component transform.

Here, we apply the Principal Component (PC) transform [20] of the fractal descriptors in the classification of the different investigated materials. Fig. 4 illustrates the ability of discrimination through BM fractal descriptors. The two classes depicted in this figure were chosen without any specific criterion and are only illustrating the discrimination power of the proposed approach. We decided not to use eight samples because in that case the data presentation will be visually confused.

The performance of the proposed approach is verified in a task of classification of titanium oxide films prepared using different experimental conditions as described in the Section 2.1. Each condition corresponds to one class.

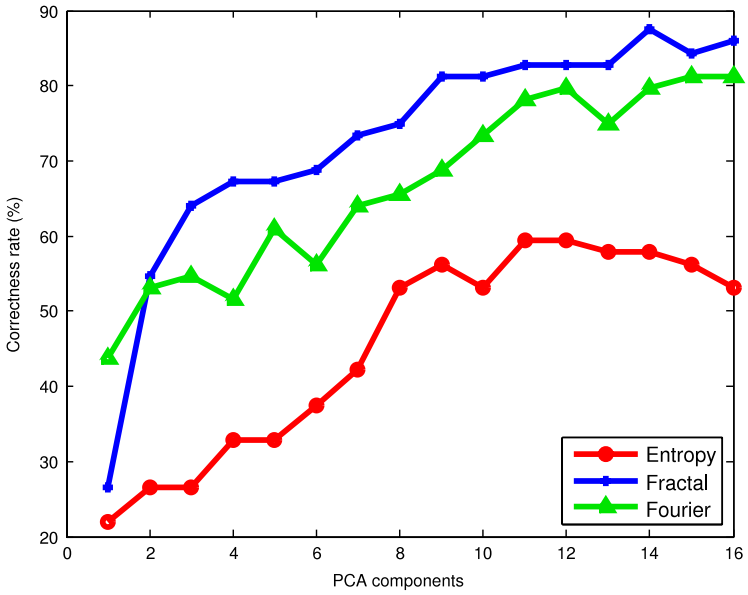

Fig. 5. Correctness rate according to the number of PC components in each compared method.

Table 2
Correctness rate for each compared descriptor.

Method	Correctness rate (%)	Number of descriptors
Entropy	59.38 ± 0.01	11
Fourier	81.25 ± 0.01	15
Fractal	87.50 ± 0.01	14

The fractal descriptors are extracted from the images and the Principal Component Analysis (PCA) is applied over each set of fractal descriptors. The components are thus classified by Linear Discriminant Analysis (LDA) [20], using leave-one-out cross-validation procedure. To check the quality of the results, they were compared to two classical texture analysis methods, that is, Fourier [21] and histogram entropy [21]. To guarantee that the comparison is valid, the same PCA–LDA methodology was applied also with these last methods.

Fig. 5 illustrates the behavior of PC components relative to their correctness rate in the classification process for each methods used. It shows the number of components up to 16 to detect the necessary number of principal components to be used.

We observe that the rate of correctness increases as the number of components increases and the Fractal descriptors achieve its maximum values faster than the other methods used. In this case, it is necessary to use 14 components. The results presented in the PC graph are summarized in the Table 2 showing the best result obtained by each descriptor, with the measure error and the number of components used to achieve such result. In this table, we changed the number of descriptors between 1 and 16 for each one of the 64 samples and each type of descriptors (entropy, Fourier and fractal) and showed the number of descriptors which achieved the best performance. After the maximum correctness, the performance decreases for every method which means that the use of more components in the LDA procedure only adds noise to the set of features, damaging the performance of the descriptors.

Now, we see that fractal descriptors showed the best correctness rate result with a 8% of advantage over the second best approach, Fourier descriptors. This result was expected due to the intrinsic ability of fractal descriptors in extracting a rich information of the topography of the surface. Such topography is directly related to important physical aspects of the material, like roughness, grain boundaries, morphologic defects, reactivity and total surface area. In this sense, we observe that the proposed descriptors are capable of accurately capturing nuances which are essential in the discrimination skill of our vision system. It is important to notice, however, that the use of descriptors associated to the classifier computational method makes the analysis of details with a complex processing framework possible which ensures a more precise and robust solution for the discrimination problem.

5. Conclusions

This work showed an application of fractal descriptors to the classification of samples of titanium oxide material under different experimental conditions.

We compared the performance of fractal to other classical texture descriptor approaches in the literature such as histogram entropy and Fourier. The results showed that the fractal approach obtained the best result, providing the most accurate classification. We verified, as expected, that fractal geometry is a powerful tool to describe such a nanoscale image. This is explained by the flexibility of fractals in modeling topographies arising from natural systems, like those present in titanium oxide samples.

The result encourages the research and enhancement of novel fractal-based approaches, applied to many challenging problems related to the discrimination and description of materials under different experimental conditions.

It is important to stress that this procedure can be used also for different natural or synthetic samples which can be found in the literature from different areas of the knowledge and particularly other types of metal oxides used as catalysts.

Acknowledgments

João B. Florindo is grateful to CNPq (National Council for Scientific and Technological Development, Brazil) for his doctorate grant (140624/2009-0). Ernesto C. Pereira and Mariana S. Sikora would like to thank the Brazilian research funding agencies CNPq and FAPESP (proc:2008/00180-0) for their financial support. Odemir M. Bruno gratefully acknowledges the financial support of CNPq (National Council for Scientific and Technological Development, Brazil) (Grant 308449/2010-0 and 473893/2010-0) and FAPESP (The State of São Paulo Research Foundation) (Grant 2011/01523-1).

References

[1] H. Masuda, K. Fukuda, Ordered metal nanohole arrays made by a two-step replication of honeycomb structures of anodic alumina, Science 268 (5216) (1995) 1466–1468.
[2] H. Masuda, M. Ohya, H. Asoh, M. Nakao, M. Nohtomi, T. Tamamura, Photonic crystal using anodic porous alumina, Japanese Journal of Applied Physics 38, Part 2 (12A) (1999) L1403–L1405.
[3] T. Yanagishita, K. Nishio, M. Nakao, A. Fujishima, H. Masuda, Synthesis of diamond cylinders with triangular and square cross sections using anodic porous alumina templates, Chemistry Letters 31 (10) (2002) 976–977.
[4] D. Kim, A. Ghicov, S.P. Albu, P. Schmuki, Bamboo-type tio2 nanotubes: improved conversion efficiency in dye-sensitized solar cells, Journal of American Chemical Society 130 (49) (2008) 16454–16455.
[5] L. Kaplan, Extended fractal analysis for texture classification and segmentation, IEEE Transactions on Image Processing 8 (11) (1999) 1572–1585.
[6] M.D. Abramoff, P.J. Magalhaes, S.J.R. Ram, Image processing with images, Biophotonics International 11 (2004) 36–42.
[7] D. Necas, P. Klapetek, Gwyddion: an open-source software for SPM data analysis, Central European Journal of Physics 10 (2012) 181–188.
[8] A.R. Backes, D. Casanova, O.M. Bruno, Plant leaf identification based on volumetric fractal dimension, International Journal of Pattern Recognition and Artificial Intelligence (IJPRAI) 23 (6) (2009) 1145–1160.
[9] O.M. Bruno, R. de Oliveira Plotze, M. Falvo, M. de Castro, Fractal dimension applied to plant identification, Information Science 178 (12) (2008) 2722–2733.
[10] J.B. Florindo, M. De Castro, O.M. Bruno, Enhancing multiscale fractal descriptors using functional data analysis, International Journal of Bifurcation and Chaos 20 (11) (2010) 3443–3460.
[11] R.O. Plotze, J.G. Padua, M. Falvo, M.L.C. Vieira, G.C.X. Oliveira, O.M. Bruno, Leaf shape analysis by the multiscale minkowski fractal dimension, a new morphometric method: a study in passiflora l. (passifloraceae), Canadian Journal of Botany-Revue Canadienne de Botanique 83 (2005) 287–301.
[12] J.B. Florindo, O.M. Bruno, Fractal descriptors in the fourier domain applied to color texture analysis, Chaos 21 (4) (2011) 1–10.
[13] B.B. Mandelbrot, The Fractal Geometry of Nature, Freeman, 1968.
[14] D. Harte, Multifractals: Theory and Applications, Chapman and Hall/CRC, 2001.
[15] E.T.M. Manoel, L. da Fontoura Costa, J. Streicher, G.B. Müller, Multiscale fractal characterization of three-dimensional gene expression data, in: SIBGRAPI, IEEE Computer Society, 2002, pp. 269–274.
[16] J.B. Florindo, M. Sikora, E. Pereira, O. Bruno, Multiscale fractal descriptors applied to nanoscale images (online), Journal of Superconductivity and Novel Magnetism (2012) 1–6.
[17] R.E. Bruns, I.S. Scarminio, B. de Baros Neto, Statistical Design—Chemometrics, Elsevier, 2006.
[18] C. Tricot, Curves and Fractal Dimension, Springer-Verlag, 1995.
[19] R. Fabbri, L.D.F. Costa, J.C. Torelli, O.M. Bruno, 2d Euclidean distance transform algorithms: a comparative survey, ACM Computing Surveys 40 (1) (2008) 1–44.
[20] R.O. Duda, P.E. Hart, Pattern Classification and Scene Analysis, Wiley, 1973.
[21] R.C. Gonzalez, R.E. Woods, Digital Image Processing, second ed., Prentice Hall, Upper Saddle River, NJ, 2002.